



Contents lists available at ScienceDirect

Journal of Great Lakes Research

journal homepage: www.elsevier.com/locate/jglr

The putative Saginaw impact structure, Michigan, Lake Huron, in the light of gravity aspects derived from recent EIGEN 6C4 gravity field model

Jaroslav Klokočník^{a,*}, Jan Kostecký^{b,c}, Aleš Bezděk^{a,d}

^a Astronomical Institute, Czech Academy of Sciences, Fričova 298, CZ 251 65 Ondřejov, Czech Republic

^b Research Institute of Geodesy, Topography and Cartography, CZ 250 66 Zdíby 98, Czech Republic

^c Faculty of Mining and Geology, VSB-TU Ostrava, CZ 708 33 Ostrava, Czech Republic

^d Faculty of Civil Engineering, Czech Technical University in Prague, CZ 166 29 Praha 6, Czech Republic

ARTICLE INFO

Article history:

Received 25 May 2018

Accepted 16 November 2018

Available online xxxx

Communicated by: Harvey Thorleifson

Keywords:

Saginaw Bay impact

Younger Dryas impact hypothesis

Gravity field model EIGEN 6C4

Gravity field aspects

Combed strike angles

ABSTRACT

The hypothetical impact structure in the Saginaw Bay (Michigan, USA, Lake Huron) has been tested by the gravity data derived from the recent gravity field model EIGEN 6C4 (expanded to degree and order 2190, with ground resolution of ~9 km). The following gravity field aspects were used: the gravity disturbances/anomalies, second derivatives of the disturbing potential (Marussi tensor), two of three gravity invariants, their specific ratio (known as 2D factor), the strike angles, and the virtual deformations. These gravity aspects are sensitive in various ways to the underground density contrasts. For the Saginaw Bay area, we confirm that we do not see any typical impact crater in terms of gravity disturbance or the radial second order derivative, possibly because of the thick layer of the ice located at the place and time of the impact. But the “combed” strike angles (one type of the gravity aspects we use) disclose a trace of high pressure to the SE/SW of the Bay and may be due to an impacting body. Thus, we provide circumstantial evidence of the Younger Dryas impact hypothesis.

© 2018 International Association for Great Lakes Research. Published by Elsevier B.V. All rights reserved.

Introduction and theory

The *Younger Dryas (YD) impact hypothesis (YDIH)* was published by Firestone and Topping (2001) and was substantially extended in their subsequent works (e.g., Firestone et al., 2007). They seek to explain the abrupt cooling after 12,900 years ago (12.9 ka), extinction of Pleistocene megafauna, and the termination of the Clovis culture. They assume that a comet or asteroid exploded over the Laurentide Ice Sheet, 1–2 km thick, around 12.9 ka ago with a huge impact on all life. But, critical voices draw attention on the lack of an impact crater, unambiguously shocked material or other features diagnostic of an impact or large chronological uncertainties (see Pinter et al., 2011 and Boslough et al., 2012, in which the reader can find many other references). The question even is whether this area, which lies south of the Mason-Quimby line, was not ice free at the time of the proposed YDIH (see discussion below). Davias and Harris (2015), among others, correlate the YD impact with Carolina Bays, oval features which have an unresolved origin. Wolbach and et al. (2018) support the YDIH with existing evidence that the YD impact event caused an anomalously large episode of biomass burning,

resulting in extensive atmospheric soot/dust loading that triggered an “impact winter.” The hypothesis is still attractive for many scientific and popular writers.

There is a good summary of evidence for a Saginaw Bay impact at the website: http://cintos.org/SaginawManifold/Saginaw_Bay/. Although their hypothesis largely depends on Carolina Bays evidence, they do reference a number of published anomalies associated with the Saginaw Bay. One suggestion is that an impact into the glacier further north created a large glacial lake that subsequently collapsed catastrophically, excavating Saginaw Bay and possibly creating the subsequent gravitational anomalies.

It is not our goal to discuss arguments supporting or refusing the YDIH. We simply add our observations using new gravity data (and using much more than the traditional gravity anomalies only), based on the global gravity field model EIGEN 6C4 (European Improved Gravity model of the Earth by New techniques, Förste et al., 2014). Such an approach has not been used for this purpose yet, so this is a novel application. With the gravity data from EIGEN 6C4, we verified quickly that the expected typical impact crater (and its gravity signal) is missing, but other gravity-derived data, (known as the gravity aspects, namely the strike angles) appear to support the YDIH.

The gravitational field of the Earth is usually described by the gravitational potential in terms of spherical harmonic expansion, the better the quality data, the higher degree and order of harmonic expansion

* Corresponding author.

E-mail address: jklokocn@asu.cas.cz (J. Klokočník).

possible, which provides more details and a higher resolution of the gravity field. A set of harmonic coefficients in the spherical expansion represents a so-called *gravity field model*; this is the input data for all our analyses.

Our knowledge about the Earth gravity field, combined from a huge amount of diverse satellite and terrestrial data, has increased substantially during the last two decades, in precision as well as in resolution. Thus, various geo-applications of these data, previously impossible, are now feasible. We make use of the recent gravity field model EIGEN 6C4, expanded in spherical harmonics (Stokes parameters) to degree and order 2190, yielding a ground resolution of ~9 km. From the Stokes parameters, we compute a set of functions, sometimes very complicated, and they show specific, often typical character for the impact structures, volcanoes, mountain ranges, lakes, underground water, faults, deposits of minerals, etc. With this method, we have confirmed, for example, paleolakes under the sands of Sahara already known to geologists (Klokočník et al., 2017a), we predicted two candidates for subglacial volcanoes in east Antarctica near Lake Vostok (Klokočník et al., 2017c), three subglacial lakes and one lake basin between the Gamburtsev Subglacial Mountains and Lake Vostok (Klokočník et al., 2018a) and confirmed a giant impact structure in Wilkes Land (Klokočník et al., 2018b). We also have discovered symptomatic gravity signals for known large oil&gas deposits (Klokočník and Kostelecký, 2015).

Here, we apply the same approach (the set of gravity aspects), well tested before for other objects, for the putative impact crater in Saginaw Bay. We emphasize that we make use of more “gravity aspects” (functions of EIGEN 6C4 potential) than only the gravity anomalies which was very helpful and finally led us to support the YDIH. But we use only the gravity data, and other data types, for example magnetic anomalies, would be also useful.

The position of the Saginaw Bay and the surface topography of the surrounding area is given in Fig. 1. It is based on the ETOPO 1 satellite topography model; it is a 1-arcmin (cell size) global relief model of the Earth surface that integrates land topography and ocean bathymetry (Amante and Eakins, 2009). Precision is 10–20 m in height depending on locality. Fig. 1 has contour lines in the interval of 50 m. The topographical area is mostly flat.

Gravity studies applied to geoscience usually employed only the traditional gravity anomalies (or gravity disturbances), sometimes also second (radial) derivatives of the disturbing potential. It is more complicated to compute the second derivatives (more precisely the whole Marussi tensor) than the gravity anomalies only; but, if used, they provide a more complete information about the underground causative body (density anomaly) than the gravity anomaly itself. The information from the Marussi tensor is not only about the position of the underground body, but also about its shape and orientation. We work with a set of functions of the disturbing gravitational potential with different attributes, so-called “gravity aspects”. These are the following: the gravity anomaly (or disturbance) Δg , second derivatives of the disturbing potential (T_{ij}) known as Marussi tensor (Γ), namely its radial component T_{zz} , two of three gravity invariants (I_j), their specific ratio I , the strike angles θ and the virtual deformations vd . These gravity aspects are sensitive in various ways to the underground density contrasts (variations) (Klokočník et al., 2016), demonstrating that the gravity anomalies are related to deeper density anomalies while the invariants and other gravity aspects are related to shallowly deposited density changes. In order to obtain a more complete picture, we compute and use *all* the gravity aspects listed above.

The theory comes from Pedersen and Rasmussen (1990), Beiki and Pedersen (2010) and from our own papers Kalvoda et al. (2013) and Klokočník et al. (2016, 2017b), in which the reader can find all the formulae, as only a selection of these are repeated here.

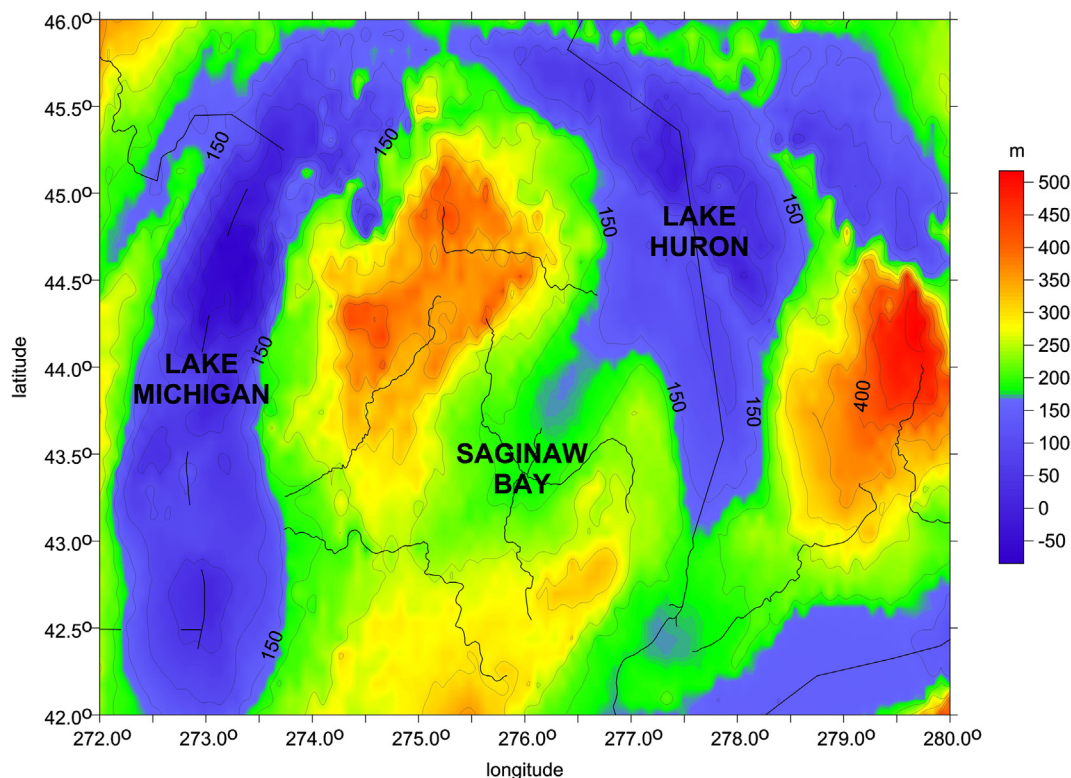


Fig. 1. The topography of the studied area, based on the ETOPO 1 model. The SW end of the Bay has geodetic latitude 43°39' N and longitude 276°10' E. [The longitudes are from 0 to 360° in the east direction of Greenwich.]

One of the gravity aspects is the *strike angle* θ (also known as strike lineaments or strike direction); it is defined as

$$\tan 2\theta = 2 \frac{T_{xy}(T_{xx} + T_{yy}) + T_{xz}T_{yz}}{T_{xx}^2 - T_{yy}^2 + T_{xz}^2 - T_{yz}^2} = 2 \frac{-T_{xy}T_{zz} + T_{xz}T_{yz}}{T_{xz}^2 - T_{yz}^2 + T_{zz}(T_{xx} - T_{yy})} \quad (1)$$

within a multiple of $\pi/2$.

Let us recall that the Marussi tensor consisting of the second derivatives of the disturbing potential is defined (in a given coordinate system not defined here) as

$$\Gamma = \begin{bmatrix} T_{xx} & T_{xy} & T_{xz} \\ T_{yx} & T_{yy} & T_{yz} \\ T_{zx} & T_{zy} & T_{zz} \end{bmatrix} \quad (2)$$

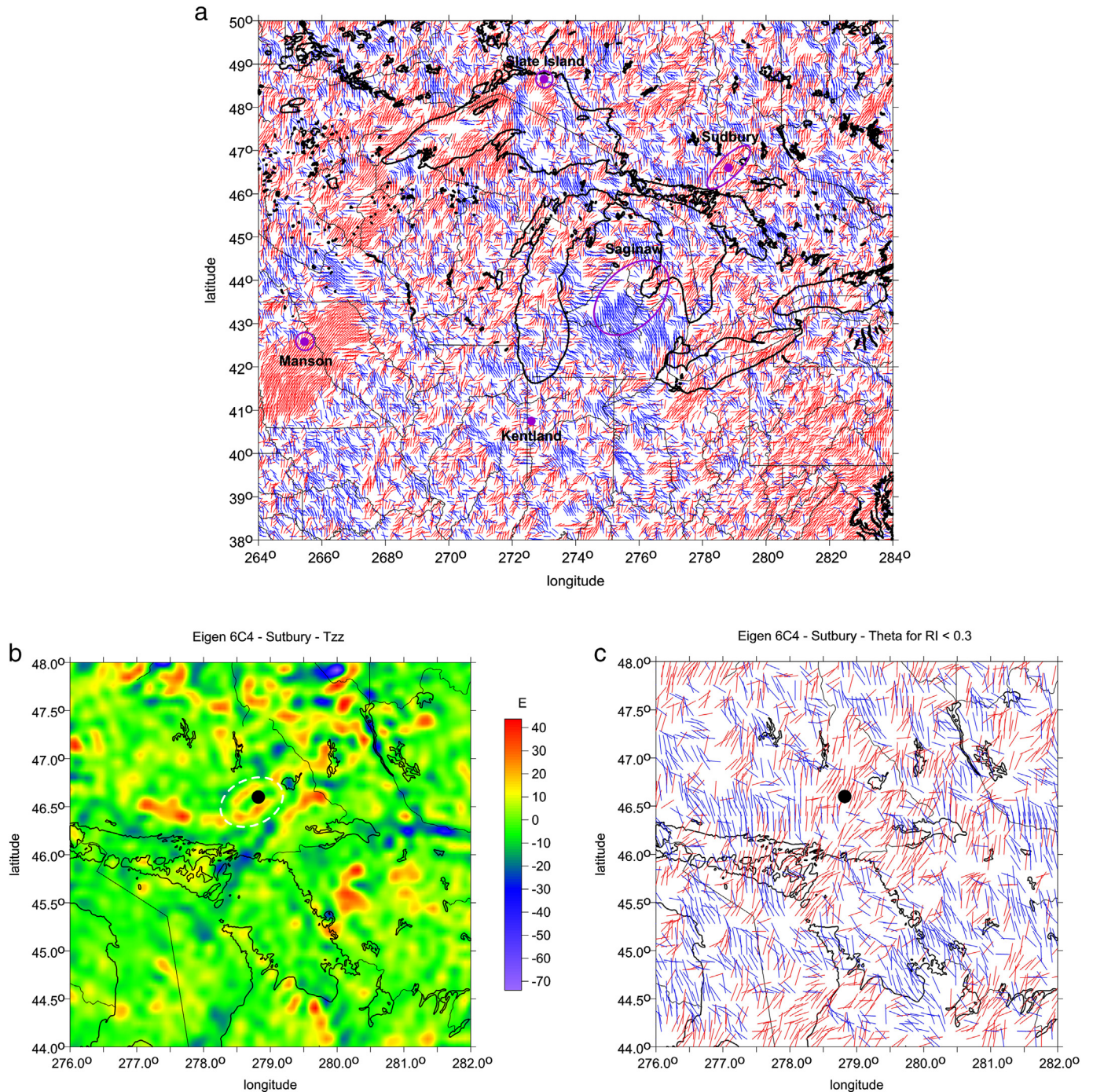


Fig. 2. Top: The Great Lakes Area with θ . The position of the known impact craters Sudbury, Slate Island, Manson, and Kentland are shown together with the Saginaw Bay structure. Middle: Details of T_{zz} [E] for the Sudbury area (note effect of Wanapitei impact in lake east of Sudbury). The negative value at the center of the structure (see black dot) is surrounded by a positive belt of elliptical shape. A similar result is for Δg (not shown here). Bottom: Details of θ , [°] for the Sudbury area; one can see combed θ , in and near the crater, oriented roughly S-N. It is uncertain what is connected with the crater and what outside the crater belonging to some other structure.

The strike angle θ shows the main direction of Γ ; this is the direction of the underground structure (the causative body with a density contrast with respect to the surrounding structures).

A usual situation is that the strike angles θ have diverse directions; they look chaotic. The *combed strike angles* are the strike angles oriented roughly in one and the same direction in a given area. It is not so important which direction it is, but the unidirectionality is important. The possible reasons for “being combed” are mentioned below.

The gravity invariants are just three. The first invariant I_0 , known as Laplace equation, is the sum of the components of (2) on the main diagonal and outside the masses of the Earth’s body equals zero. The other two invariants are non-linear combinations of the components of the Marussi tensor of the second derivatives of the disturbing potential:

$$I_1 = (T_{xx}T_{yy} + T_{yy}T_{zz} + T_{xx}T_{zz}) - (T_{xy}^2 + T_{yz}^2 + T_{xz}^2) = \sum_{(i,j) \in \{x,y,z\}} (T_{ii}T_{jj} - T_{ij}^2) \quad (3)$$

$$I_2 = \det(\Gamma) = (T_{xx}(T_{yy}T_{zz} - T_{yz}^2) + T_{xy}(T_{yz}T_{xz} - T_{xy}T_{zz}) + T_{xz}(T_{xy}T_{yz} - T_{xz}T_{yy})) \quad (4)$$

where *det* means determinant of Γ .

Pedersen and Rasmussen (1990) showed that the ratio I of the invariants I_1 and I_2 , defined as

$$0 \leq I = -\frac{\left(\frac{I_2}{2}\right)^2}{\left(\frac{I_1}{3}\right)^3} \leq 1 \quad (5)$$

is always between zero and one for any potential field. If the causative body is strictly 2D (flat), then I is equal to zero; the higher I , the “more 3D” causative object, according to the theory.

The second order derivatives and the invariants provide evidence about the details of near-surface (not deep) structures. The Marussi tensor was already used locally (areas of a few kilometres) for petroleum, metal, diamond, groundwater, and other explorations (e.g., Saad (2006), Mataragio and Kieley (2009), Murphy and Dickinson (2009), and many others). The full Marussi tensor is a rich source of information about the density anomalies providing useful details about the underground objects located closely to the Earth’s surface and their orientation.

To define the “virtual deformations” (originally defined in Kalvoda et al., 2013 and Klokočník et al., 2014) (*vd*), an analogy with the tidal deformation was utilized; one can imagine directions of such a deformation due to a tension, “erosion”, brought about solely by “gravity origin”. To illustrate *vd*, the semi-axes of deformation ellipse are

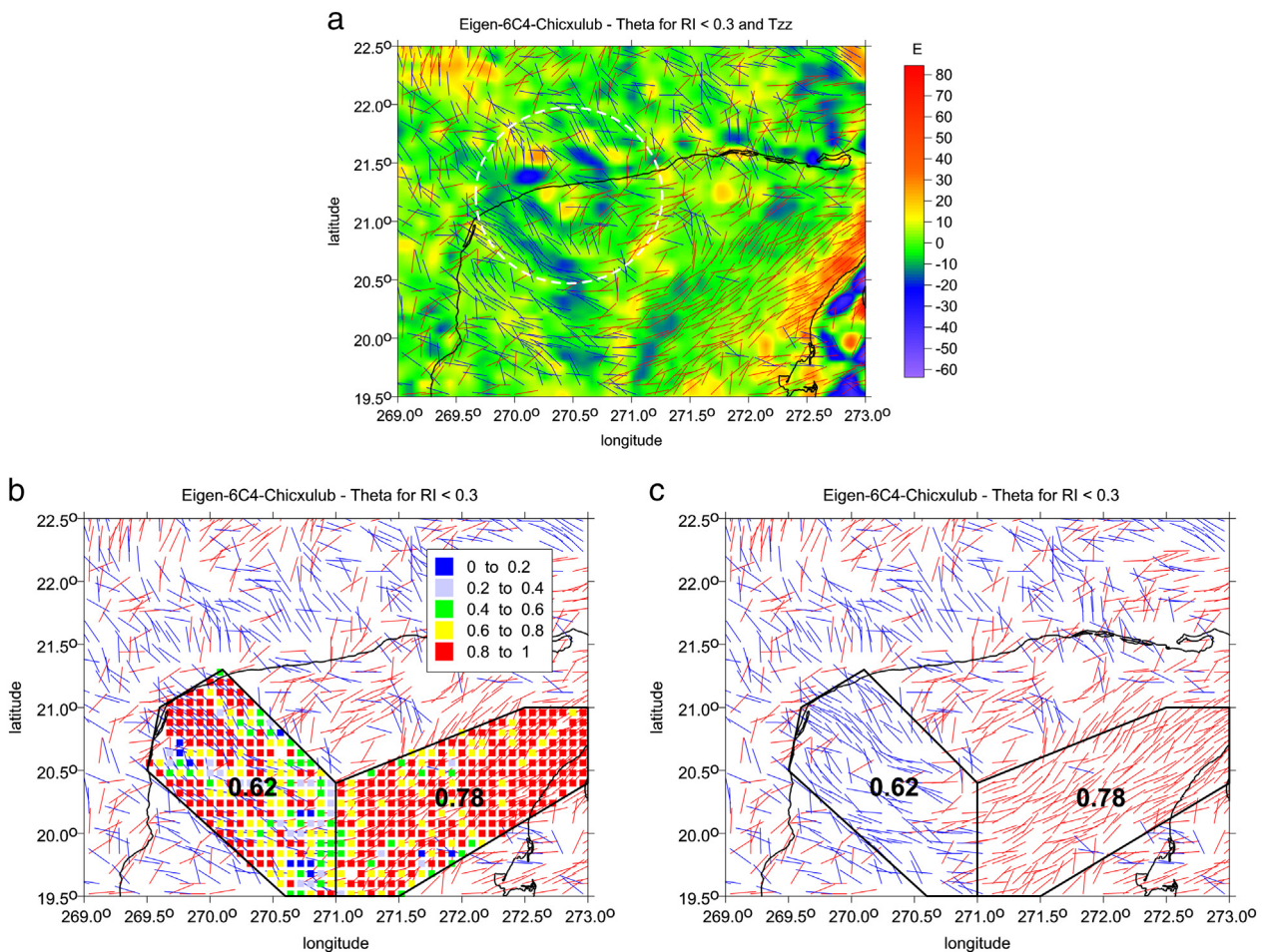


Fig. 3. a) Area of the Chicxulub impact structure on the Yucatan Peninsula, Mexico. Black line is the shoreline of the Yucatan Peninsula south of the Gulf of Mexico. Strike angles are superimposed over the second radial derivative T_{zz} [E]. They show a central positive value and rings with positive values and negative values in between. The strike angles θ [–] are combed mainly outside the central part of the structure (SE and E areas), partly also inside the crater following its round shape (but this is well visible only in the part of the crater under the land, not under the sea). b) Chicxulub structure on Yucatan Peninsula, combed strike angles and the values θ_i^{flat} in small pixels in two parts of the studied area. c) The *Comb* factor at the Chicxulub area reaches 0.78.

computed together in their relative size. The vd is geometrically expressed by its dilatation (in our figures shown in red colour) or compression (in blue). The virtual dilatation indicates uplifted regions at the geoid, whose mass has a tendency to disintegrate (owing or according to the pattern of values of the gravitational potential), whereas the virtual compression indicates lowered zones at the geoid.

The colour figures presented here have non-linear scales to emphasize various features and details. The gravity disturbances (anomalies) are given in milliGals [$mGal$], the second order derivatives are in Eötvös [E]. Recall that $1 mGal = 10^{-5} ms^{-2}$, $1E \equiv 1 Eötvös = 10^{-9} s^{-2}$ and that the invariants have units $I_1 [s^{-4}]$ and $I_2 [s^{-6}]$. The strike angle θ in all figures is expressed in degrees with respect to the local meridian (north-south direction): the red arrows indicate its direction to the west and those in blue to the east. We computed and prepared all relevant figures of θ in this paper for $I < 0.3$.

Theory and examples of combed strike angles

The theory

As mentioned above, the combed strike angles are strike angles oriented roughly in one and the same direction. We define the combed coefficient $Comb$ for the strike angles θ as a relative value in the interval $(0, 1)$, where 0 means “not combed” (the vectors θ are in diverse directions) and 1 “combed” (perfectly kempt, the vectors of θ are oriented into one prevailing direction).

These are the input data:

$$\theta_i \in (-90^\circ, 90^\circ), \quad i = 1, \dots, n$$

for n pixels in the studied area or zone. We compute the main direction of “combing” as a mean value of θ_i ; let us denote it as θ_{Comb} :

$$\theta_{Comb} = \frac{\sum_{i=1}^n \theta_i}{n}$$

by choosing the angles θ_i either in the interval $(-90^\circ, 0^\circ)$ or in the interval $(0^\circ, 90^\circ)$.

We use the following important condition:

$$\forall (|\theta_i - \theta_{Comb}| > 90^\circ) : \theta_i = 180^\circ - |\theta_i|$$

which means that even two angles θ_i in the opposite directions are counted as one direction.

For example: for $\theta_{Comb} = 80^\circ$ and $\theta_i = -80^\circ$, a deviation from the main $Comb$ direction is 20° .

Let us define a root mean square value of scatter (variance) of θ_i for n pixels as:

$$rmsv = \sqrt{\frac{\sum_{i=1}^n (\theta_i - \theta_{Comb})^2}{n}}$$

Then the required value of the main $Comb$ direction can be defined as

$$Comb = 1 - \frac{rmsv}{90^\circ}$$

As a measure of degree of θ “being combed” (the combed factor), in our plots we make use of the relative values of θ_i :

$$\theta_i^{relat} = 1 - \frac{abs(\theta_i - \theta_{Comb})}{90^\circ} \tag{6}$$

So the $Comb$ value is the main local direction of the tested set of θ_i of the given region; the departures of the individual θ_i from $Comb$ are plotted in a preselected optimum size of n rectangular pixels in a relative

scale; these are the values of (6); if some of θ_i fits to the main direction $Comb$, then the pixel has value 1; if not, then the values (6) are in the interval $(0, 1)$. This serves for a simple statistical evaluation to compare the areas with combed to those with “non-combed” strike angles. If $Comb$ is smaller than 0.55, we say that θ_i of the given region are “not combed”; if $Comb > 0.65$, we say θ_i are “combed”; there is a “grey zone” in between $Comb = 0.55-0.65$.

For the impact craters, we always (at least for larger objects, where our resolution is sufficient) observe the combed θ_i , but sometimes the vectors θ_i have a tendency to follow the crater’s ring(s), thus they are of circular shape and the $Comb$ statistics is not appropriate. Sometimes the combed θ_i are inside the crater, sometimes outside it. Sometimes the reason for being combed in that area can be a combination of more factors (the impact structure, oil or gas deposits, underground water nearby). We have to be aware of it. The gravity information is not unambiguous. A few examples with craters of various size and age follow.

Crater examples

We have previously discovered a correlation between places of combed strike angles and known large deposits of oil, gas or underground water (Klokočník and Kostelecký, 2015; Klokočník et al., 2018a, 2018b) Also the impact craters reveal combed and “rotating” θ .

First we show the Great Lakes Area with θ_i in Fig. 2a. [Note that all figures are based on computations with the gravity field model EIGEN 6C4]. The position of the known impact craters Sudbury (oval shape, ~130 km), Slate Island (30 km in diameter), both in Ontario (Canada), Manson (35 km in diameter) in Iowa, and Kentland (13 km in diameter, on a limit of the resolution of EIGEN 6C4) in Indiana are shown. The Saginaw Bay is added. The strike angles are significantly combed at Saginaw (for more details see Fig. 7a–d), but also at the other larger craters. The

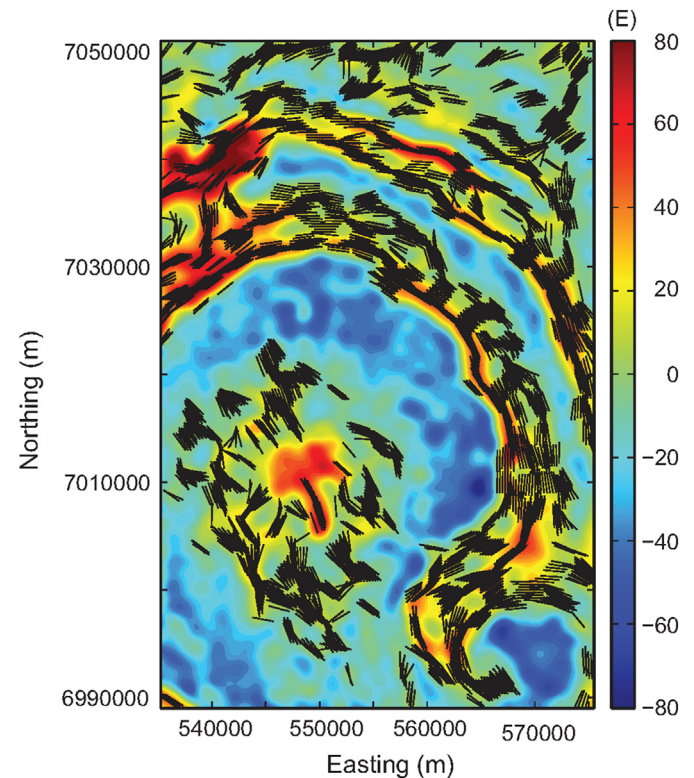


Fig. 4. The strike angles follow rings of the impact structure Vredefort, South Africa. In the central part of the crater they are more or less combed. To draw this, Beiki and Pedersen (2010) used the detailed local airborne gradiometry data, which we have not available and the resolution of our data source (EIGEN 6C4) is not sufficient for this purpose. (Easting and Northing are coordinates in a specific rectangular coordinate system, not geodetic latitude and longitude used for other figures in this paper).

large combed area at Manson in Iowa can be connected with the crater but also with gas deposits. The details (T_{zz} and θ_i) for Sudbury are shown in Fig. 2b, c; one can see clearly combed strike angles.

Another example is in Fig. 3a; it is for the large impact crater Chicxulub on the Yucatan Peninsula, Mexico (diameter 170–250 km), not visible on the surface, buried under 1 km of sediments, partly beneath a flat land, partly in a shallow sea. The strike angles are superimposed over T_{zz} . In the SE and E areas of the structure, θ are

significantly combed, see Fig. 3b, c for the *Comb* factor, rotating their direction around the central crater. The combed θ look better preserved under the land than under the sea; it is not clear why. The question is what part of the combed θ belongs to the crater and what (in the SE and E directions) may already be influenced by something else (Campeche Bank oil deposit, for example).

The strike angles perfectly follow the craters rings in the case of Vredefort (~300 km in diameter), South Africa. This is shown using

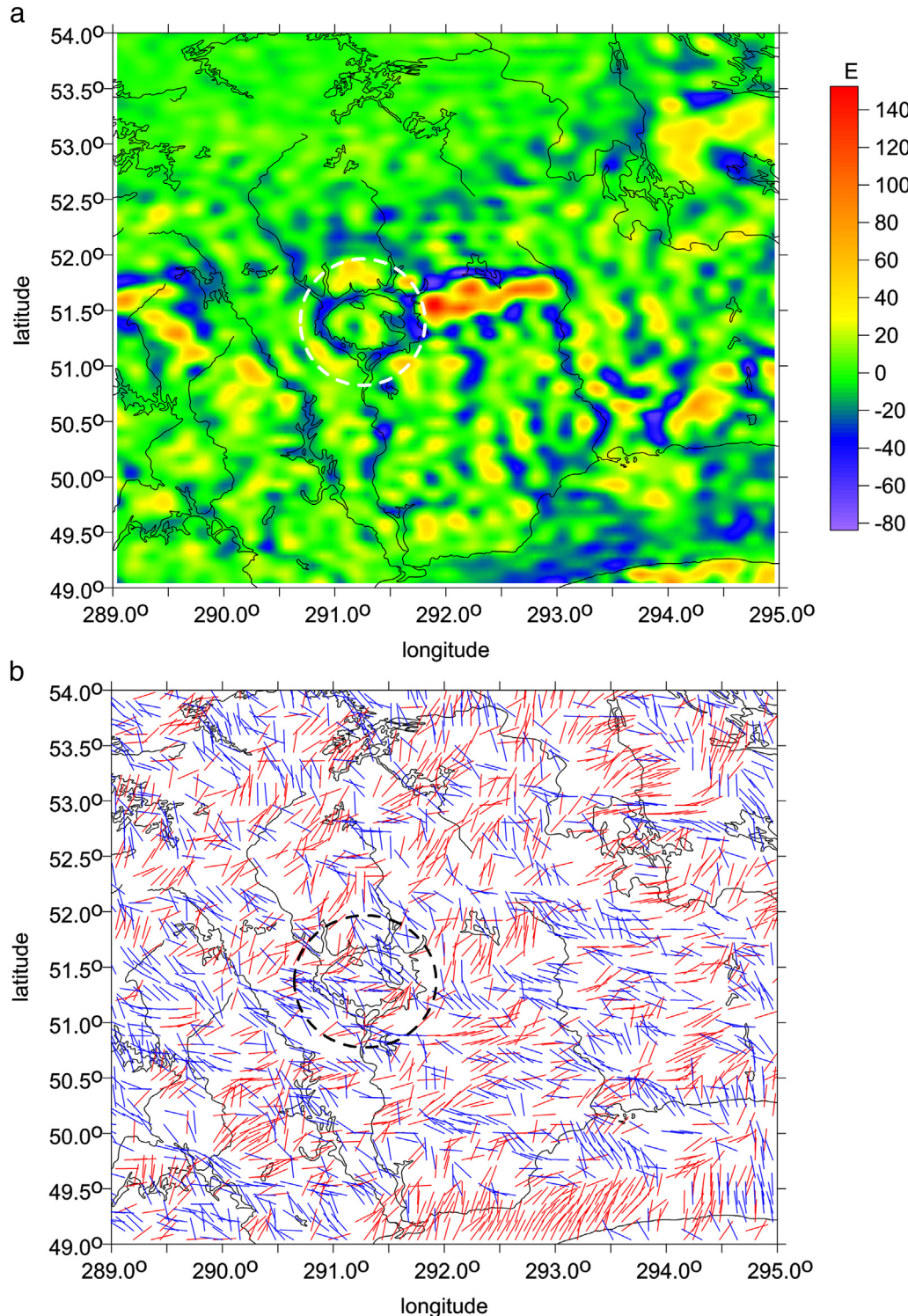


Fig. 5. a) T_{zz} [E] for the Manicouagan crater. b) θ_i [-] for the Manicouagan crater. One can see a trend of θ_i to follow the ring around the crater, but we have to account our limited resolution ~10 km.

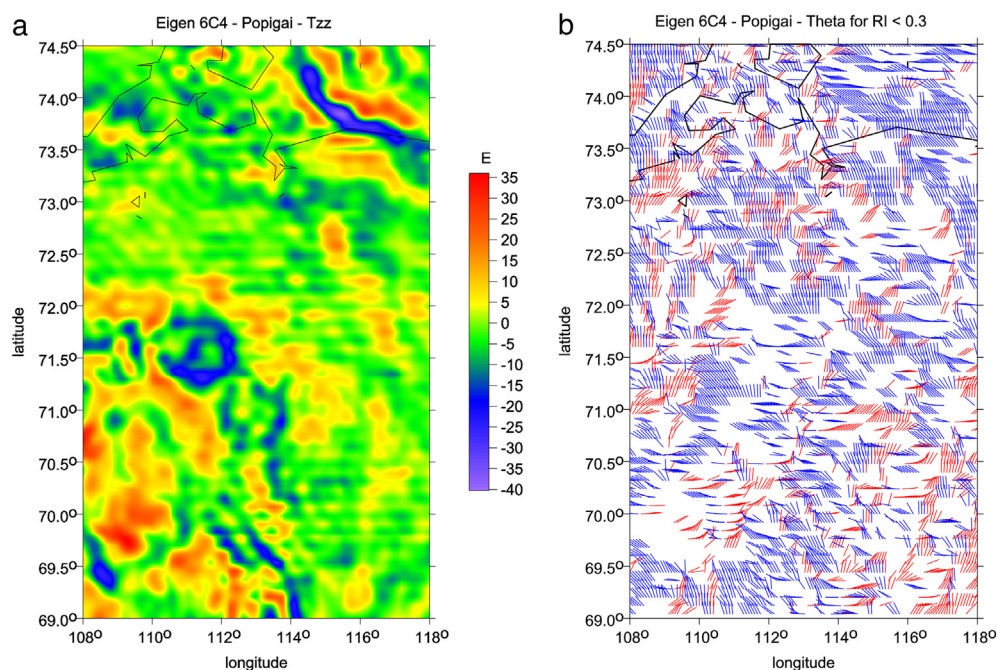


Fig. 6. a) T_{zz} [E] for Popigai crater. b) θ_i [-] for the Popigai.

the detailed local (not satellite, but airborne) gradiometry data in Fig. 11d in Beiki and Pedersen (2010); we reproduce it here as Fig. 4. At our resolution, given by the gravity field model EIGEN 6C4,

i.e., about 10 km on the ground, we have no chance to see such details. With EIGEN 6C4, we can see very fragmented Δg , T_{zz} , θ_i or vd (not shown here).

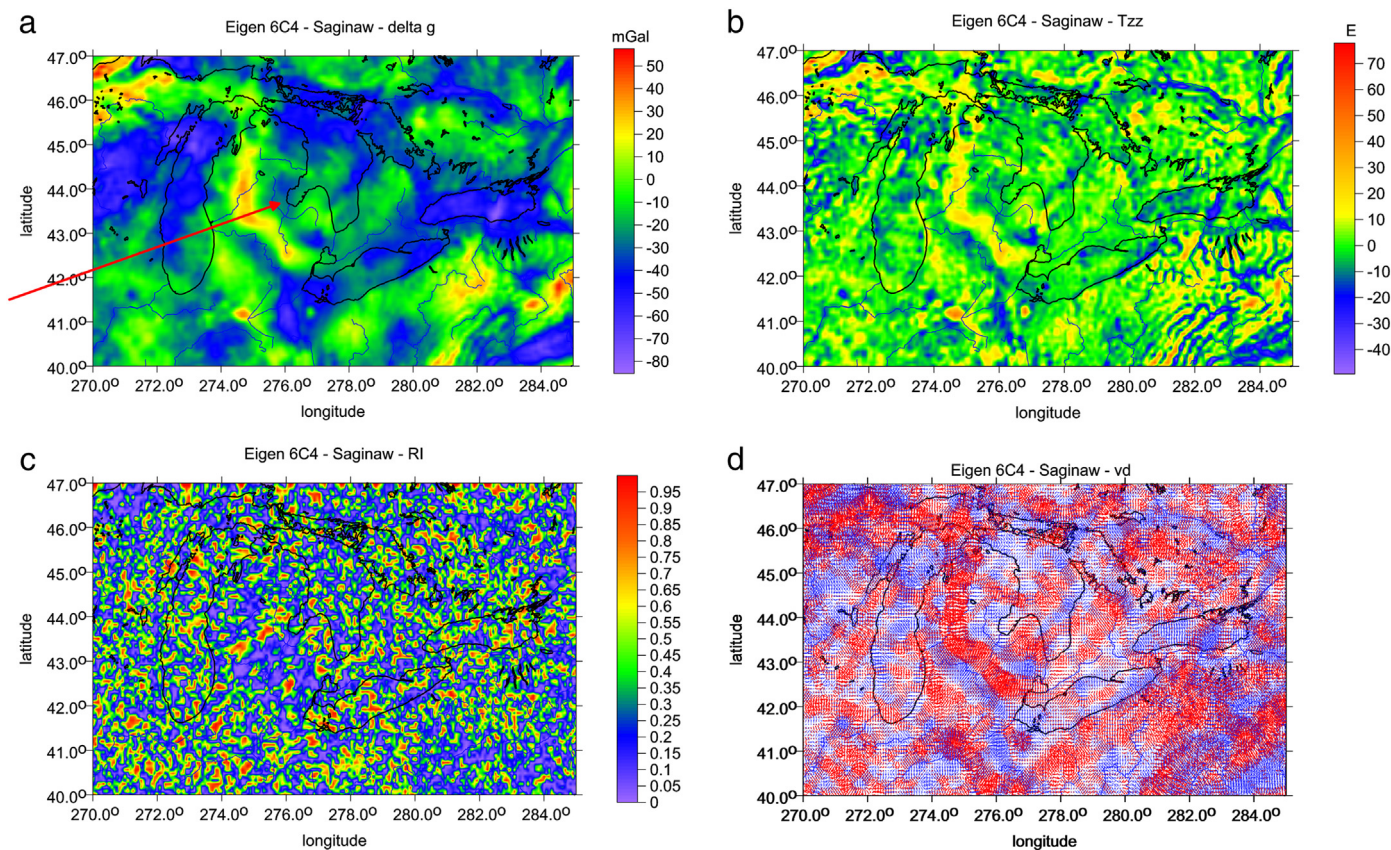


Fig. 7. a) The gravity disturbances Δg [mGal] for the studied area of the Great Lakes with Saginaw Bay (red arrow), using EIGEN 6C4. b) The second radial derivative T_{zz} [E] for the studied area of the Great Lakes with Saginaw Bay, using EIGEN 6C4. c) The ratio of the invariants I [-] for the studied area of the Great Lakes (black outline) with Saginaw Bay, using EIGEN 6C4. d) The virtual deformations vd [-] for the studied area of the Great Lakes with Saginaw Bay, using EIGEN 6C4 (dilatation in red, compression in blue). (For interpretation of the references to colour in this figure legend, the reader is referred to the web version of this article.)

In Fig. 5a, b we present T_{zz} and θ_i for the Manicouagan Reservoir (~100 km in diameter) in Canada. The T_{zz} values delineate the crater ring, filled by water. One can see also a trend of θ_i to follow the ring around the crater, but again, we have to recall our resolution limit.

In Fig. 6a, b we present T_{zz} and θ_i for the Popigai crater (~100 km in diameter) in Siberia, Russia. Note that this crater may be a multiple crater (Klokočník et al., 2010), with components lined up in SW-NE direction and with negative T_{zz} inside the crater and partly fragmented positive T_{zz} in the rim around it. As for the strike angles θ_i , they are here also combed but located asymmetrically around the crater's center.

This asymmetry is observed often in or around impact structures. We speculate about a relationship between the field of stresses indicated somehow by the combed θ_i and the fall direction of the impactor. Not too much is known about the conditions of the impact, e.g., the projectile mass, speed, impact angle, etc. The currently most frequently used method for estimating the direction and obliquity of impact is based on the observed pattern of crater ejecta, but they may be missing and the oval shape of the crater today may result from subsequent tectonic processes after the impact. For further studies see, e.g., Ormö et al. (2013) with many references to older works. This topic needs a further investigation.

Although many questions about this novel approach using the gravity aspects and namely the strike angles to identify impact structures remain to be answered, we documented on the examples of known impact structures that the strike angles connected with such structures are combed or follow the crater's ring(s). This knowledge can be utilized for the Saginaw structure.

The main input data and computations

The input data to our analysis are the harmonic geopotential coefficients (also known as Stokes parameters) in the spherical harmonic expansion of the disturbing gravitational potential. A set of these coefficients is known as a static global gravitational (gravity) field model. We make use of a high resolution model EIGEN 6C4, to degree and order (d/o) 2190; this corresponds to a resolution of 5×5 arc minutes (~9 km half-wavelength on the Earth's surface).

GOCE satellite with gradiometer (Gravity and steady state Ocean Circulation Explorer, e.g., ESA, 2014), measuring directly the component of

the Marussi tensor, was an important source for improvement of EIGEN 6C4 (but, as always in the case of satellite data, the most important for the long(er) wavelength part of the gravity model, say below d/o ~250). The higher degree/order harmonics come mostly from terrestrial gravimetry (Pavlis et al., 2012). This is taken into EIGEN 6C4 mostly from the US EGM 2008 global gravity field model (Pavlis et al., 2012).

The computation of all gravity aspects from EIGEN 6C4 is done by software based on Bucha and Janák (2013) and by our own software. We ensure numerical stability of the higher derivatives to very high degrees. The results of this method has been presented for different parts of the world in different ways (Kalvoda et al., 2013; Klokočník et al., 2014; Klokočník and Kostecký, 2015), including the confirmation of existence of paleolakes under the sands of Sahara (Klokočník et al., 2017a) or subglacial volcanoes and lakes in Antarctica (Klokočník et al., 2016, 2017c, 2018a).

Results for a putative Saginaw Bay impact structure

A typical impact crater has a negative Δg and T_{zz} inside the crater's body, with a possible positive central peak in T_{zz} and positive Δg and T_{zz} in the rims around the center and a negative Δg and T_{zz} between them. Typical vd are negative inside the crater (compression) with a positive belt(s) (dilatation) around it. The values of θ can be combed. Nothing extra is visible in the invariants, and the ratio I tends to be low inside the crater.

For the Saginaw Bay impact, we do not see any typical impact crater, possibly because of the thick layer of ice at the place and time of the putative impact. We show Δg and T_{zz} for the studied area in Fig. 7a, b, and I and vd in Fig. 7c, d.

Provided that the correct location of the impact is as shown in Fig. 2a, we have to say that Fig. 7a, b exhibit local minima of Δg and T_{zz} on the expected place but north-east and south-west parts are divided by positive belts; this is not a typical gravity signal of any impact crater. Similarly for vd in Fig. 7d. Then, Fig. 7c exhibits a low ratio I (blue area), but again not in all the area shown in Fig. 2a.

If the position of the impact in Figs. 1 and 2a is not correct, we can seek for a crater nearby using the same gravity aspects. It is also possible that the impact crater is smaller than expected and only for example the

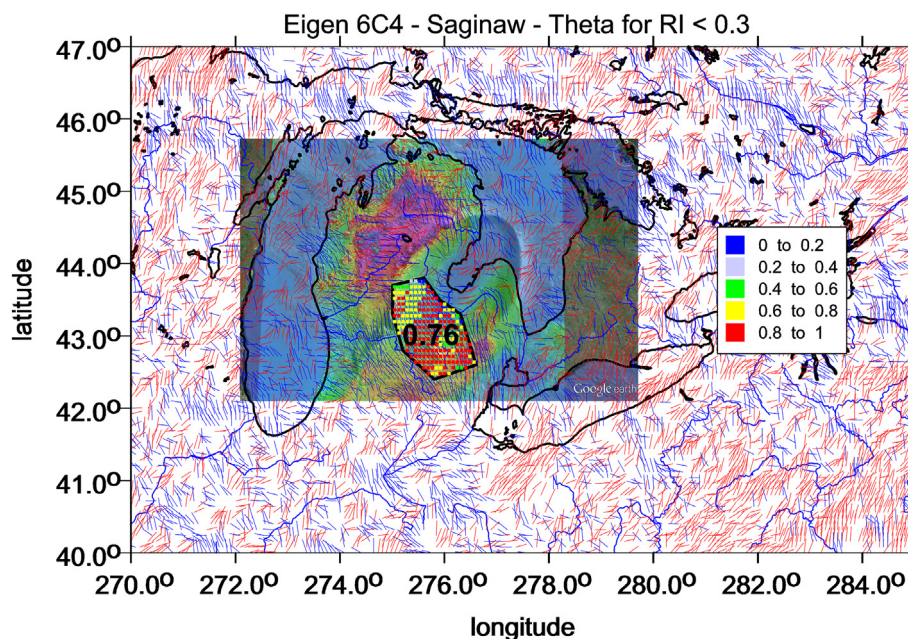


Fig. 8. The combed strike angles θ_i [—] for the studied area of the Great Lakes specifically in the Saginaw Bay, using EIGEN 6C4, with the Comb statistics (0.76). Superposed over a figure from Davias and Harris (2015).

northern negative part of Δg and T_{zz} belongs to it. The gravity data themselves are not unambiguous to decide it, but they can help us.

If the area of a hypothetical impact place was ice-free at that time, then we can consider the impact in water, with a similar damping and other effects. But this is just a speculation. We studied an attenuation of Δg and T_{zz} under the ice of Antarctica (Klokočník et al., 2018a). It can be compared with dumping by water; a dumping of Δg in ice in various situations may reach tens of percent of the signal on free air; a reduction of T_{zz} is not significant.

The strike angles θ in the Saginaw Bay (Fig. 2a) are well combed. In Fig. 2a, it looks like they rotate a bit around the SW and S end of the putative crater. Recalling previous figures, this is a positive indication of an impact event, a possible trace of high pressure due to the impacting body.

It is important to note that this was revealed by means of one of the gravity aspects and that this effect might hardly be discovered only with the traditional Δg .

Conclusion

The hypothetical impact crater in the Saginaw Bay (the Great Lakes area), has been studied from various views. Here, we used the recent gravity field model EIGEN 6C4 and a set of gravity aspects (sensitive in various ways to the underground density contrasts), derived from its spherical harmonic coefficients (Stokes parameters) to degree and order 2190, with a ground resolution of ~9 km.

We do not see any typical impact crater related to the putative Saginaw Bay impact in terms of Δg and T_{zz} , possibly because of a thick layer of ice at the place and time of the impact. But the strike angles θ are well combed (oriented more or less in one direction). This may be a trace of high pressure due to the impacting body (Fig. 8). For this reason, we do not write 'a requiem for the Younger Dryas impact hypothesis' (see Pinter et al., 2011). At the beginning of our analyses of YDIH, our attitude to this hypothesis was neutral. After the analyses, we provide circumstantial evidence of it and cautiously support it. We present a new approach, based on recent, high quality gravity data and on the use of a set of the gravity aspects, which is not widely applied yet; thus it is novel. With the traditional gravity anomalies only, we would not discover anything new.

Acknowledgments

This work has been prepared in the frame of project RVO #679 858 15 (Czech Academy of Sciences), partly supported by the project LO 1506 (PUNTIS) from the Ministry of Education of the Czech Republic.

References

Amante, C., Eakins, B.W., 2009. ETOPO1, 1 arc-minute global relief model: procedures, data sources and analysis. NOAA Techn. Memo. NESDIS NGDC-24. National Geophysical Data Center, NOAA <https://doi.org/10.7289/V5C8276M>.

Beiki, M., Pedersen, L.B., 2010. Eigenvector analysis of gravity gradient tensor to locate geologic bodies. *Geophysics* 75, 137–149. <https://doi.org/10.1190/1.3484098>.

Boslough, M., Nicoll, K., Holliday, V., Daulton, T.L., Meltzer, D., Pinter, N., Scott, A.C., Surovell, T., Claeys, P., Gill, J., Paquay, F., Marlon, J., Bartlein, P., Whitlock, C., Grayson, D., Jull, A.J.T., 2012. Arguments and Evidence Against a Younger Dryas Impact Event. *Geophysical Monograph Series* 198, pp. 13–26. <https://doi.org/10.1029/2012GM001209>.

Bucha, B., Janák, J., 2013. A MATLAB-based graphical user interface program for computing functionals of the geopotential up to ultra-high degrees and orders. *Comput. Geosci.* 56, 186–196. <https://doi.org/10.1016/j.cageo.2013.03.012>.

Davies, M.E., Harris, T.H.S., 2015. A tale of two craters: coriolis-aware trajectory analysis correlates two pleistocene impact strewn fields and gives Michigan a thumb. *GSA North-Central Section Meeting, Madison, WI 19 May, 20, Paper 3-1, Session T 10*.

ESA, 2014. GOCE High Level Processing Facility, GOCE Level 2 Product Data Handbook, Doc. GO-MA-HPF-GS-0110, pp. 21–23. <https://earth.esa.int/web/guest/missions/esa-operational-eo-missions/goce>.

Firestone, R.B., Topping, W., 2001. Terrestrial evidence of a nuclear catastrophe in Paleolithic times. *Mammoth Trumpet* 16 (2), 9–16.

Firestone, R.B., West, A., Kennett, J.P., Becker, L., Bunch, T.E., Revay, Z.S., Schultz, P.H., Belgica, T., Kennett, D.J., Erlandson, J.M., Dickenson, O.J., Goodyear, A.C., Harris, R.S., Howard, G.A., Kloosterman, J.B., Lechler, P., Mayewski, P.A., Montgomery, J., Poreda, R., Darrach, T., Hee, S.S.Q., Smith, A.R., Stich, A., Topping, W., Wittke, J.H., Wolbach, W.S., 2007. Evidence for an extraterrestrial impact 12,900 years ago that contributed to the megafaunal extinctions and the Younger Dryas cooling. *Proc. Natl. Acad. Sci. U. S. A.* 104, 16,016–16,021. <https://doi.org/10.1073/pnas.0706977104>.

Förste, Ch., Bruinsma, S., Abrykosov, O., Lemoine, J.-M., et al., 2014. The latest combined global gravity field model including GOCE data up to degree and order 2190 of GFZ Potsdam and GRGS Toulouse (EIGEN 6C4). 5th GOCE User Workshop, Paris 25–28, Nov.

Kalvoda, J., Klokočník, J., Kostecký, J., Bezděk, A., 2013. Mass distribution of Earth landforms determined by aspects of the geopotential as computed from the global gravity field model EGM 2008. *Acta Univ. Carolinae, Geographica, XLVIII*, 2, Prague.

Klokočník, J., Kostecký, J., 2015. Gravity signal at Ghawar, Saudi Arabia, from the global gravitational field model EGM 2008 and similarities around. *Arab. J. Geosci.* 8, 3515–3522. <https://doi.org/10.1007/s12517-014-1491-y> (ISSN 1866-7511, Springer-Verlag).

Klokočník, J., Kostecký, J., Pešek, I., Novák, P., Wagner, C.A., Sebera, J., 2010. Candidates for multiple impact craters?: Popigai and Chicxulub as seen by the global high resolution gravitational field model EGM08. *Solid Earth* 1, 71–83. <https://doi.org/10.5194/se-1-71-2010> (See also: Is Chicxulub a double impact crater? Pres. at 6th EGU A. von Humboldt Internatl. Conf. on Climate Change, Natural Hazards, and Societies, Mérida, México, Section: The Cretaceous/Tertiary Boundary and the Chicxulub Impact Crater; paper AVH6-5, 15 March 2010).

Klokočník, J., Kalvoda, J., Kostecký, J., Eppelbaum, L.V., Bezděk, A., 2014. Gravity Disturbances, Marussi Tensor, Invariants and Other Functions of the Geopotential Represented by EGM 2008, *ESA Living Planet Symp.* 9–13 Sept. 2013, Edinburgh, Scotland. Publ. in: August 2014: JESR (J Earth Sci. Res.). vol. 2 pp. 88–101.

Klokočník, J., Kostecký, J., Bezděk, A., 2016. On feasibility to detect volcanoes hidden under ice of Antarctica via their "gravitational signal". *Ann. Geophys.* 59 (5), S0539. <https://doi.org/10.4401/ag-7102>.

Klokočník, J., Kostecký, J., Čilek, V., Bezděk, A., Pešek, I., 2017a. A support for the existence of paleolakes and paleorivers buried under Saharan sand by means of "gravitational signal" from EIGEN 6C4. *Arab. J. Geosci.* <https://doi.org/10.1007/s12517-017-2962-8> (on-line).

Klokočník, J., Kostecký, J., Bezděk, A., 2017b. *Gravitational Atlas of Antarctica. Series Springer GeophysicsSpringer Nature, Book 978-3-319-56639-9 (113 pp)*.

Klokočník, J., Kostecký, J., Bezděk, A., Pešek, I., 2017c. Candidates for volcanoes under the ice of Antarctica detected by their gravito-topographic signal. *Ann. Geophys.* 60 (6), S0661. <https://doi.org/10.441/ag-7427>.

Klokočník, J., Kostecký, J., Čilek, V., Bezděk, A., Pešek, I., 2018a. Gravito-topographic signal of the Lake Vostok area, Antarctica, with the most recent data. *Polar Sci.* <https://doi.org/10.1016/j.polar.2018.05.002>.

Klokočník, J., Kostecký, J., Bezděk, A., 2018b. On the detection of the Wilkes Land impact crater. *Earth Planets Space* <https://doi.org/10.1186/s40623-018-0904-7>.

Mataragio, J., Kieley, J., 2009. Application of full tensor gradient invariants in detection of intrusion-hosted sulphide mineralization: implications for deposition mechanisms. *Mining Geoscience. EAGE First Break.* 27, pp. 95–98.

Murphy, C.A., Dickinson, J.L., 2009. Exploring exploration play models with FTG gravity data. 11th SAGA Biennial Techn. Meeting and Exhib., Swaziland, pp. 89–91, 16–18 Sept.

Ormö, J., Rossi, J.P., Housen, K.R., 2013. A new method to determine the direction of impact: asymmetry of concentric impact craters as observed in the field (Lockne), on Mars, in experiments, and simulations. *Meteorit. Planet. Sci.* 48 (Nr 3), 403–419. <https://doi.org/10.1111/maps.12065>.

Pavlis, N.K., Holmes, S.A., Kenyon, S.C., Factor, J.K., 2012. The development and evaluation of the earth gravitational model 2008 (EGM2008). *J. Geophys. Res.* 17 (B04406), 2012. <https://doi.org/10.1029/2011JB008916>.

Pedersen, B.D., Rasmussen, T.M., 1990. The gradient tensor of potential field anomalies: some implications on data collection and data processing of maps. *Geophysics* 55, 1558–1566.

Pinter, N., Scott, A.C., Daulton, T.L., Podoll, A., Koeberl, C., Anderson, R.S., Ishman, S.E., 2011. The Younger Dryas impact hypothesis: a requiem. *Earth Sci. Rev.* 106, 247–264. <https://doi.org/10.1016/j.earscirev.2011.02.005>.

Saad, A.H., 2006. Understanding gravity gradients - a tutorial, the meter reader. In: Van Nieuwenhuise, B. (Ed.), *The Leading Edge.* August issue, pp. 941–949.

Wolbach, W.S., et al., 2018. Extraordinary biomass-burning episode and impact winter triggered by the Younger Dryas cosmic impact ~12,800 years ago. 2. Lake, Marine, and terrestrial sediments. *J. Geol.* 126, 2. <https://doi.org/10.1086/695704>.